Transactions, SMiRT-26
Berlin/Potsdam, Germany, July 10-15, 2022
Division VIII

MAGNETIC METHODS FOR EVALUATION OF BCC AND BCT IRON FRACTIONS BELOW 0.1% IN AUSTENITE: SURFACE MAPPING AND FULL VOLUME EVALUATION

Viktor Lyamkin[1], Christian Boller[2]

[1] M.Sc., Chair of NDT and Quality Assurance (LZfPQ), Saarland University, Campus Dudweiler, 66125 Saarbrücken, Germany (viktor.lyamkin@uni-saarland.de)
[2] Prof. Dr.-Ing., Chair of NDT and Quality Assurance (LZfPQ), Saarland University, Campus Dudweiler, 66125 Saarbrücken, Germany

ABSTRACT

Austenitic stainless steels are commonly used in harsh environments, where corrosion resistance and structural integrity at elevated temperatures are essential to be maintained. Hence, many nuclear energy reactor components are made of austenitic materials, where safety relies on the material's microstructure. Since paramagnetic austenite is prone to transformation into ferromagnetic bcc/bct α' martensite, magnetic and electromagnetic methods are often used to characterize the respective volume fractions. At elevated temperatures, the amount of the deformation-induced α' martensite is substantially reduced and difficult to detect, which possess some unique challenges for magnetic methods.
Within this paper a possibility of detecting α' martensite below 0.1% volume is described. As an investigation tool, magnetic force imaging was chosen, as it provides spatially resolved information on magnetic susceptibility, which can be further interpreted as the density of ferrite and α' martensite. The results show that the main obstacle in the reliable estimation of small quantities of α' is calibration. The second problem is the inhomogeneous distribution of α' martensite and possibly a very small grain size, which has magnetic properties more similar to paramagnetism, rather than ferromagnetism.

INTRODUCTION

Austenitic stainless steels are incredibly diverse in their magnetic properties. They comprise a mixture of paramagnetic and ferromagnetic properties due to diverse crystalline structures. The 'non-magnetic' face-centered cubic iron (fcc) lattice is not stable at room temperature, but through the addition of alloying elements such as nickel, carbon, and manganese can become stable or metastable, depending on the ratio of alloying elements. Metastable austenitic stainless steels will form a distorted body-centered cubic (bcc) lattice if strained sufficiently (Rocha and Oliveira, 2009; Gauss *et al.*, 2016).

The bcc lattice generally exhibits strong ferromagnetic properties (Tavares, Fruchart and Miraglia, 2000; Das, 2014), unless the bcc grain size happens to be in a sub-micron and nano-scale size (Thompson and Oldfield, 1986). There are two important grain size divisions: ultra-fine superparamagnetic grains and stable single-domain grains. If the grain is under 20 nm diameter, depending on the shape, it is likely to go into a superparamagnetic state, where thermal fluctuations cause the magnetization to change spontaneously (Li *et al.*, 2017). As the size of the grain increases, the magnetization becomes stable but does not vary yet across the grain – hence a single domain structure. The critical size for a single-domain grain also depends on the shape and generally is below a micrometer in diameter (Muxworthy and Williams, 2015). If the grain increases further in size, the single-domain state faces an increasing energy cost due to the rising demagnetizing field (Morrish and Yu, 1955). Only at this point does material, as a bulk, start to show typical ferromagnetism, with magnetic wall movement as the main way to change the bulk magnetization.

The reader should get an idea by now of the challenges associated with the magnetic estimation of very small quantities of bcc grains in fcc base material: in some cases, a small volume fraction may also mean small grain size. Small grain size means different magnetic properties. In other words, the grains' size can be large, but localized only in certain areas. It is less of a challenge to quantify low concentrations in liquids, as the blend can be mixed or brought to thermal equilibrium. In solids, however, this is unfortunately not possible. This means one has to be prepared to deal with a potentially inhomogeneous distribution of small particles in a solid.

There are several suitable methods listed in the ASTM standard "Standard Test Methods for Permeability of Feebly Magnetic Materials" (ASTM A 342/A 342M-99, 2000), that are meant for estimation of susceptibility of weakly magnetic materials. Other methods include numerous force balances, such as Gouy and Faraday balances, vibrating sample magnetometer, Kappabridge, and others. In this paper, the possibility of examining ferrite and α' martensite fractions are examined with Magnetic Force Imaging (MFI) (Lyamkin, Starke and Boller, 2020).

MAGNETIC FORCE IMAGING

The MFI technique is based on the measurement of the force that acts upon a magnetic tip, as illustrated in Fig. 1. This force is the result of the interaction between the magnetic tip and the material. The magnetic tip used in this study is a permanent NdFeB cylindrical magnet with a 0.3 mm diameter. The magnetic field at the tip can be estimated to be around 300 mT.

A relatively strong magnetic field generated by the magnetic tip is capable of locally magnetizing the material to a (near) saturation state. In this case, the measured force can be related to the magnetic permeability of the material and as such can be calibrated to the ferrite fraction (Talonen, Aspegren and Hänninen, 2004; Putz et al., 2019).

The calibration to relative permeability was done with linear approximation, between $\mu_r = 1.37$ (carbonyl iron powder) and $\mu_r = 1.00$ (air). The calibration to the ferrite fraction was accomplished with 0.64 Fe%, 1.78 Fe%, and 11.7 Fe% calibration samples from Helmut Fischer GmbH. Within this range, the relationship between the magnetic force and the ferrite fraction was found to be linear.

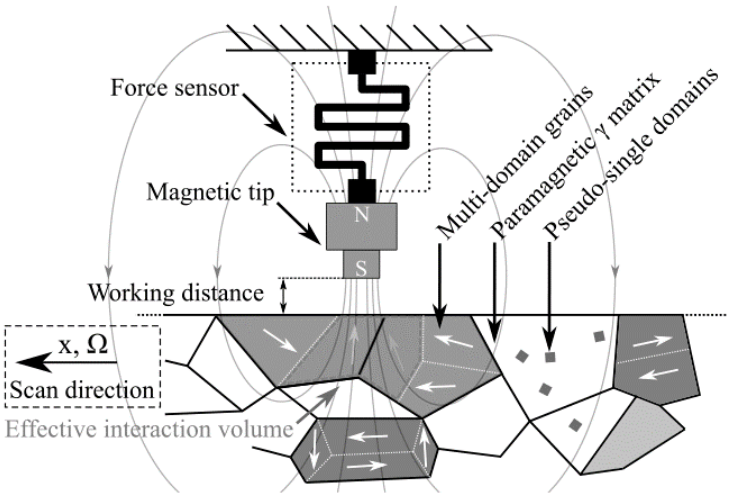

Figure 1. Schematic illustration of the magnetic force scanning principle (Lyamkin, Starke and Boller, 2020).

CHALLENGES OF ESTIMATING FRACTIONS BELOW 0.1%

Chemical and microstructural inhomogeneity

One of the main aspects that makes evaluation of small fractions of α' martensite difficult is that the density of α' is not necessarily homogeneous within the given volume, especially in metastable austenitic steels. The reasons for that can be small variations in chemical composition or grain structure that are almost unavoidable in production of parts with a low surface-to-volume ratio. This creates regions in austenite that are more susceptible to γ → α' transformation than the others.

As an example, Fig. 2 illustrates the distribution of α' in commercially available X6CrNiNb18-10 (AISI 347) steel. The bar was analyzed in an 'as-delivered' condition, without additional heat treatment. A fairly high concentration of α' was detected in the outer surface of the bar, which comes from turning of the specimen to the final 30 mm diameter (Fig. 2b).

The rectangular shape in the center (Fig. 2a) is the inheritance of the manufacturing process, where first the material is cast in a rectangular shape and later formed into a round bar. Relative permeability

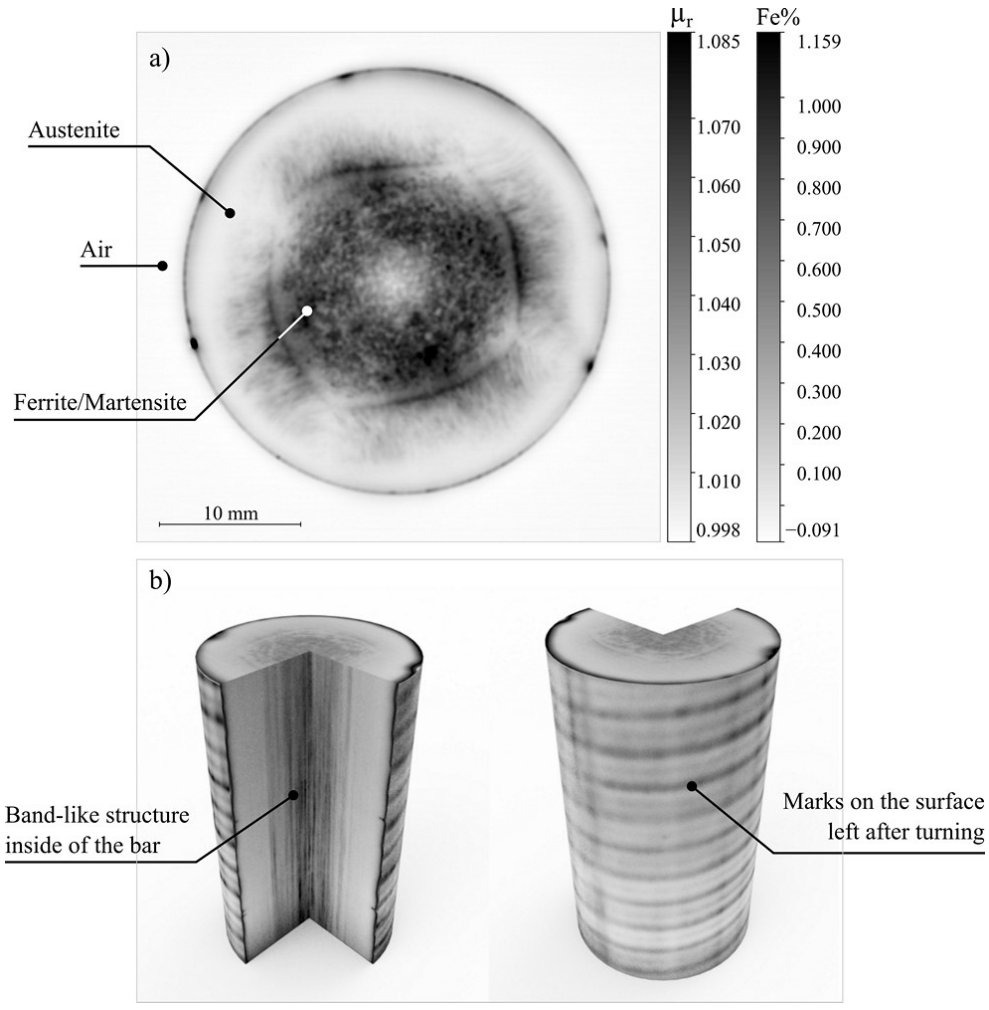

Figure 2. X6CrNiNb18-10 bar in as-delivered condition from the manufacturer: a) MFI scan of the radial section of the bar; b) a composed image from radial, longitudinal, and rotary scans of the bar. The grayscale in b) does not correspond to a). The surface in a) was polished with 6, 3, and 1 μm diamond suspension after sandpaper grinding in water.

readings indicate here a definite presence of the ferromagnetic phase in the material. However, depending on the location of the measurement, very different values can be obtained. This variation is linked to the varying density of α'. After calibrating the MFI reading to the ferrite volume fraction (Fe%), the variation spans between 0.1 Fe% to 1 Fe%. Should the same sample be measured not with a spatially-resolving method, a misleading interpretation of the microstructural composition can be attained.

Interpretation of the ferrite reading below 0.1%, obtained by a magnetic susceptibility measurement, is not straightforward. Since this, and many other methods heavily rely on calibration, a standard of pure austenite with similar chemical composition is required to achieve accurate results. But in the case of metastable alloys, this can be a challenge. Additionally, α' martensite can be incredibly small, down to the single-digit nm range (Shimojo et al., 2001). Such a small size with a combination of a very low density makes it difficult to detect with diffraction methods and non-homogeneous distribution makes it difficult to quantify with electron microscopy.

The calibration problem

The lowest reading in Fig. 2 around $\mu_r = 1.005$ can be found approximately 5 mm from the sample edge. The question here: Is this pure austenite or is there still a tiny fraction of α' martensite. When the force response of MFI is calibrated to the relative magnetic permeability, the output in the lower range is calibrated to μ_r of air which is equal to 1.00000037 (Cullity and Graham, 2009). Since the measured value is in between μ_r of air and $\mu_r = 1.37$ of the standard calibration sample, a higher degree of accuracy can be achieved compared to the calibration to ferrite fraction. The problem with calibration to the Fe% is the lack of a standard sample below 0.1 Fe%. Unlike with relative permeability, air cannot be used as a zero Fe% reference point since the magnetic susceptibility of pure austenite is much higher compared to air. The values of relative magnetic permeability μ_r for fully annealed austenitic steels found in the literature vary typically between 1.003 and 1.009 (Chinzei, Kikinis and Jolesz, 2006; Sukhon et al., 2010).

A set of ferrite calibration samples offered by Helmut Fischer GmbH includes 0.64 Fe%, 1.78 Fe%, and 11.7 Fe% samples. The force reading of MFI was found to be linear within this range. However, it is not possible to make an accurate prediction of the ferrite reading below 0.1% due to a large scatter within the standard samples. Fig. 3 shows the MFI scan of the 0.64 Fe% standard sample. One can observe around 10% deviation in the ferrite reading within 14 x 12 mm^2 scanned area. To achieve an accurate calibration, a standard sample with 0.01 %Fe or less would be needed. Since such samples are not readily available, a work-around method was used to estimate the Fe% reading in Fig. 4: a lower band estimation of austenite permeability $\mu_r = 1.002$ was used as a zero reference for calibration to the ferrite reading. The second point for calibration was the average reading from the 0.64 Fe% sample.

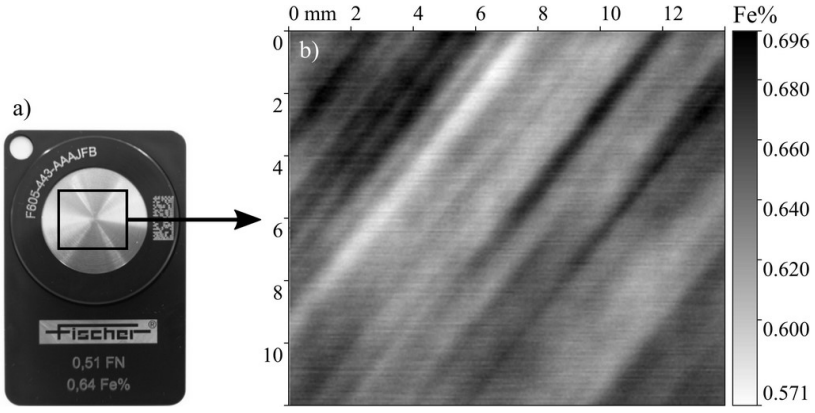

Figure 3. A standard calibration sample from Fischer, 0.63% ferrite or 0.51 ferrite number (FN): a) the standard sample and the scanned area; b) MFI scan of the calibration sample.

The material in Fig. 4 is X6CrNiTi1810S in the fully annealed condition, 10 mm thick. Great care was taken to avoid the formation of deformation-induced α' martensite during grinding. The polishing was done with a diamond suspension of 6 µm followed by 3 and 1 µm. As one can see, the magnetic response of the material is not entirely homogeneous. A certain magnetic structure of higher and lower density can be observed in the entire sample. When calibrated to relative magnetic permeability, the values on the surface were found to be between 1.002 and 1.007.

Since this material is known to have α' martensite rather than ferrite, a further conversion might be needed. Below 30% vol., readings of ferrite were found to be convertible to α' martensite by applying a factor of 1.7 to the ferrite reading (Fava et al., 2018). However, this factor should also be used with caution, as magnetic properties of α' martensite are quite diverse due to the large scatter in the possible grain sizes. The observed fraction of α' martensite in Fig. 4 calibrated to the ferrite fraction appear to deviate between 0.01% and 0.08%, which is likely to be the lower measurement limit. Applying the 1.7 factor these fractions change to 0.017% and 0.136%, respectively. Further metallographic research is needed to confirm the accuracy of this approach.

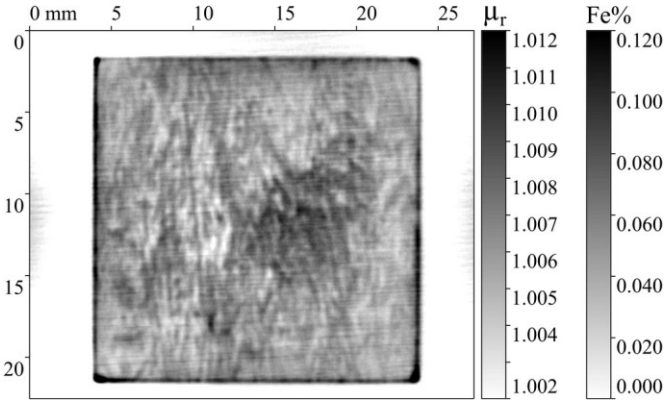

Figure 4. MFI scan of X6CrNiTi1810S in the fully annealed condition. The surface was polished with 6, 3, and 1 µm diamond suspension after sandpaper grinding in water.

CONCLUSIONS

This paper is meant to present the challenges associated with the estimation of α' martensite and ferrite fractions in austenite below 0.1% vol.. α' martensite can form fairly small sized grains, which in a combination of very low density makes it difficult to be detected with diffraction methods and a non-homogeneous distribution makes it additionally difficult to quantifiy with electron microscopy. Magnetic methods are generally more sensitive, but to achieve accurate results a very careful examination of the data is needed.

It has been shown with magnetic force imaging how inhomogeneous the distribution of α' martensite in metastable austenitic steels can be. Calibration was found to be the main obstacle for the reliable estimation of small quantities of α'. To achieve a reasonable calibration for ferrite volume fraction determination, relative permeability $\mu_r = 1.002$ was taken as a zero ferrite volume calibration point. Further metallographic investigations are needed to confirm the accuracy of this assumption. The second challenge in the estimation of ferrite and α' martensite fractions was found to be the inhomogeneous distribution within the volume and extremely diverse grain sizes, which substantially changes the magnetic properties of the material.

ACKNOWLEDGMENTS

This research is part of the project "Life cycle estimation of metallic components in nuclear industry based on non-destructive detection and interpretation of local material properties" sponsored by the Federal Ministry for Economic Affairs and Energy (Bundesministerium für Wirtschaft und Energie).

REFERENCES

ASTM A 342/A 342M-99 (2000) *Standard Test Methods for Permeability of Feebly Magnetic Materials*, *ASTM Standard*.

Chinzei, K., Kikinis, R. and Jolesz, F. (2006) 'MR Compatibility of Mechatronic Devices: Design Criteria', in *Lecture Notes in Computer Science*. doi: 10.1007/10704282_111.

Cullity, B. D. and Graham, C. D. (2009) *Introduction to Magnetic Materials*. John Wiley & Sons, Inc.

Das, A. (2014) 'Magnetic properties of cyclically deformed austenite', *Journal of Magnetism and Magnetic Materials*. North-Holland, 361, pp. 232–242. doi: 10.1016/J.JMMM.2014.02.006.

Fava, J. O. *et al.* (2018) 'Assessment of the amount of deformation induced martensite: a calibration curve for a commercial delta-ferrite gauge', *12th European Conference on Non-Destructive Testing (ECNDT 2018), Gothenburg 2018, June 11-15 (ECNDT 2018)*, (1), pp. 1–8.

Gauss, C. *et al.* (2016) 'In situ synchrotron X-ray evaluation of strain-induced martensite in AISI 201 austenitic stainless steel during tensile testing', *Materials Science and Engineering A*. Elsevier, 651, pp. 507–516. doi: 10.1016/j.msea.2015.10.110.

Li, Q. *et al.* (2017) 'Correlation between particle size/domain structure and magnetic properties of highly crystalline Fe3O4 nanoparticles', *Scientific Reports*. Nature Publishing Group, 7(1), pp. 1–7. doi: 10.1038/s41598-017-09897-5.

Lyamkin, V., Starke, P. and Boller, C. (2020) 'Magnetic force imaging for spatially resolved assessment of ferromagnetic phase fraction in austenitic stainless steel', *Journal of Magnetism and Magnetic Materials*, 497. doi: 10.1016/j.jmmm.2019.165973.

Morrish, A. H. and Yu, S. P. (1955) 'Dependence of the Coercive Force on the Density of Some Iron Oxide Powders', *Journal of Applied Physics*, 26, p. 1049. doi: 10.1063/1.1722134.

Muxworthy, A. R. and Williams, W. (2015) 'Critical single-domain grain sizes in elongated iron particles: implications for meteoritic and lunar magnetism', *Geophysical Journal International*. Oxford Academic, 202(1), pp. 578–583. doi: 10.1093/GJI/GGV180.

Putz, A. *et al.* (2019) 'Methods for the measurement of ferrite content in multipass duplex stainless steel welds', *Welding in the World*. Springer Berlin Heidelberg, 63(4), pp. 1075–1086. doi: 10.1007/s40194-019-00721-4.

Rocha, M. R. da and Oliveira, C. A. S. de (2009) 'Evaluation of the martensitic transformations in austenitic stainless steels', *Materials Science and Engineering A*, 517(1–2), pp. 281–285. doi: 10.1016/j.msea.2009.04.004.

Shimojo, M. *et al.* (2001) 'Formation of nanosized martensite particles in stainless steels', *Metallurgical and Materials Transactions A 2001 32:2*. Springer, 32(2), pp. 261–265. doi: 10.1007/S11661-001-0257-9.

Sukhon, R. *et al.* (2010) 'A study on volumetric magnetic susceptibility of weight due to its manufacturing process', *21st Conference on Measurement of Force, Mass and Torque Together with HARDMEKO 2010 and 2nd Meeting on Vibration Measurement, IMEKO TC3, TC5 and TC22 Conferences*, d(November 2010), pp. 303–306.

Talonen, J., Aspegren, P. and Hänninen, H. (2004) 'Comparison of different methods for measuring strain induced α-martensite content in austenitic steels', *Materials Science and Technology*, 20(12), pp. 1506–1512. doi: 10.1179/026708304X4367.

Tavares, S. S. M., Fruchart, D. and Miraglia, S. (2000) 'A magnetic study of the reversion of martensite α' in a 304 stainless steel', *Journal of Alloys and Compounds*, 307, pp. 311–317.

Thompson, R. and Oldfield, F. (1986) *Environmental Magnetism*. Allen&Unwin Ltd, UK.